Polarization selection with stacked hole array metamaterial

M. Beruete, M. Navarro-Cía, M. Sorolla, and I. Campillo

Additional information on J. Appl. Phys.

Polarization selection with stacked hole array metamaterial

M. Beruete,[1,a)] M. Navarro-Cía,[1,b)] M. Sorolla,[1,c)] and I. Campillo[2,d)]

[1]*Millimeter Wave Laboratory, Universidad Pública de Navarra, E-31006 Pamplona, Spain*
[2]*CIC nanoGUNE Consolider, Paseo Mikeletegi 56, 301, 20009 Donostia, Spain*

Polarization rotation or selection appears in materials with optical activity, or those with Faraday effect, or in liquid crystals. In this letter we present a structure, with an analogous response, using stacked extraordinary transmission subwavelength hole arrays modified to be nearly self-complementary. This produces a polarization selector because of the negative index of refraction for one of its linearly polarized eigenwaves. Simulation results and experiments at millimeter wavelengths confirm these features. Applications in miniaturized devices are envisioned as well as the possibility to scale to optical wavelengths. © *2008 American Institute of Physics*.
[DOI: 10.1063/1.2841471]

I. INTRODUCTION TO POLARIZATION AND LEFT-HANDED METAMATERIALS

The polarization of a plane wave is defined as the direction of the electric field oscillation in a plane transverse to the propagation. Light polarization is relevant in theoretical physics because of the similitude between the formalisms describing elliptically rotating electromagnetic field vectors and spin properties of particles.[1] Polarization is also useful in many areas of scientific research, such as astronomy, chemistry, and biology. Moreover, the ability to isolate a specific polarization state has given a lot of technological applications, such as photography, antennas, communication systems, and modern liquid crystal display (LCD) screens.[2–4]

Some natural materials, which have molecules with a helical aspect, cause polarization rotation, that is usually referred to as optical activity. Other materials have similar response when an external magnetic field is applied, the so-called Faraday effect.[3,4] Also, twisted nematic liquid crystals behave as an optically inhomogeneous anisotropic medium that resembles locally a uniaxial crystal with its optical axis parallel to the direction of the molecules.[3]

A general view of these effects are the bianisotropic media where each **D** and **H** fields are given as a linear combination of **E** and **B** fields multiplied by 3×3 matrices. When the above matrices are replaced by nonzero scalars we deal with biisotropic media, that include the so-called Chiral media.[2,4] In all these media, the eigenwaves are not linearly polarized waves but circularly polarized ones. Therefore, an impinging linearly polarized wave needs to be described by a superposition of right- and left-handed circularly polarized waves with different wavenumber values. As the waves propagate inside the medium they acquire different phase delays which cause the rotation of the polarization.[2]

In Ref. 5, it is proposed the use of chiral metamaterial designs to avoid the need of two sets of resonant structures, one for the electric and the other for the magnetic response,

requiring a complex design to obtain both resonances at the same frequency. As it can be expected, the introduction of a single chiral resonance produces the negative refraction effect only in one of the polarizations. These chiral structures could alleviate the big problem of metamaterial losses at optical wavelengths.

In this letter, we face this problem in a fresh perspective, which involves negative and positive refraction propagation indices for each eigenwave. Moreover, it should be noted that in our case the eigenwaves are linearly polarized and, therefore, a simplified alternative viewpoint to the chiral design of Ref. 5 is opened up sharing the advantages of chiral metamaterials for the problem of the design of both resonances at the same frequency and the fact that negative refraction effect appears only in one of the polarizations.

Hence, we get another degree of freedom to fix the phase difference and, furthermore, virtually any polarization can be obtained at the output with an intuitive design. The proposed structure is based on previous results of stacked extraordinary transmission hole arrays.

The discovery of extraordinary transmission (ET) phenomenon through subwavelength hole arrays[6] stimulated the research activities in this topic opening up, simultaneously, technological applications.[7] Initially, the phenomenon was reported at optical wavelengths,[6] but it was also proven in the millimeter wave range.[8–10] A general explanation of the phenomenon at different electromagnetic ranges can be found in Ref. 11.

Besides, it has been shown the possibility to obtain a left handed metamaterial (LHM) by just stacking several perforated plates showing ET at subterahertz wavelengths,[12,13] and at optical frequencies.[14,15] It was also demonstrated that the LHM propagation through such structures can be inhibited by means of a photonic band Gap[13] (PBG) and, also, that a zero group band can be achieved.[13] It is very remarkable that ET, LHM, and PBG are linked phenomena that can be found in the same structure. Furthermore, it has been very recently demonstrated[16] that a stacking of double-period self-complementary hole arrays behaves, at normal incidence, as a negative refractive index (NRI) medium for the linearly polarized vertical (E_y) component, whereas the linearly

---

a)Electronic mail: miguel.navarro@unavarra.es
b)Electronic mail: miguel.beruete@unavarra.es
c)FAX: +34948169720. Electronic mail: mario@unavarra.es
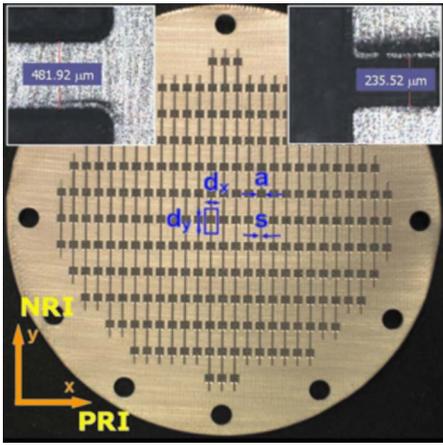d)Electronic mail: i.campillo@nanogune.eu

FIG. 1. (Color online) Photograph of the fabricated structure. Parameters: $d_x = 1.8$ mm, $d_y = 3.8$ mm, $a = 1.2$ mm, $s = 0.2$ mm. Substrate parameters: relative dielectric constant $\epsilon = 2.43$, thickness $h = 0.49$ mm, metal thickness $t = 35$ μm, and conductivity $\sigma = 5.8 \times 10^7$ S/m. Insets show details of the fabrication.
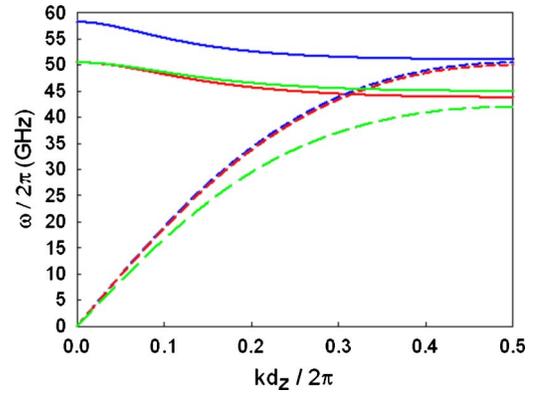

FIG. 2. (Color online) Computed dispersion diagram particularized to the primary band of each polarization: NRI (solid curves) and PRI (dashed curves), for different transversal lattices. The longitudinal lattice of the stack is $d_z = 0.525$ mm in all cases.

polarized horizontal component is inhibited. Here we report how this kind of structures shows optical activity. It is interesting to note that very recently it has been shown the suitability to manipulate the polarization states by means of reflections onto an anisotropic metamaterial plate[17] in contrast with the transmission approach presented in our work.

II. ANALYSIS AND DESIGN OF A LEFT-HANDED AND RIGHT-HANDED METAMATERIAL FOR EACH ORTHOGONAL POLARIZATIONS

The proposed structure consists of the stacking of the self-complementary extraordinary transmission structures shown in Fig. 1. It will be shown below that the parameters of the screen can be modified, logically deviating a bit from an ideal self-complementary structure, to allow propagation on both axes, with negative or positive refraction indices in the vertical and horizontal components, respectively [for notation convenience, from this point on the copolar direction will be referred as NRI axis and the cross polar as positive refraction index (PRI) axis]. Simulation and experimental results will be presented showing the polarization selection and rotation capabilities of the structure.

The phase difference φ between polarization components can be adjusted with the length of the structure through the relation

$$\varphi = (\beta_+ + |\beta_-|)(N-1)d_z, \qquad (1)$$

where N is the number of stacked plates, d_z is the longitudinal stack period, and β_+ and β_- are the wavenumbers of the PRI and NRI eigenwaves, respectively. In the arrangement $d_z \ll \lambda$, therefore, practically any desired phase difference can be obtained by just stacking plates. Also, notice that the phase difference progression is very fast since now the phase components add due to the minus sign of the NRI component. Then, comparatively thinner polarizers than those based on incremental rotations in multiple inclined wire gratings can be obtained.[1]

Theoretically, the polarizer is able to rotate a linear polarization to the orthogonal one. For instance, a vertically

polarized wave at the input with the polarizer rotated an angle $\gamma = 45°$ and a phase difference $\varphi = 180°$, is transformed into a horizontal polarized wave at the output. If $\varphi = \pm 90°$, then the polarization at the output is circular. Also, we can switch from an input right-handed circular polarization to an output left-handed circular polarization (LHCP). In intermediate cases we have elliptical polarization.

Therefore, the structure behaves as a polarization selector providing any desired polarization at the output, with the only condition of having field components on both polarizer axes at the input. Thus, we can switch from any polarization to any other polarization.

Now a further step is given in the practical implementation of the polarizer. Using a numerical finite integration in the time domain method,[18] we calculate the dispersion diagram of the kind of structure shown in Fig. 1, see Fig. 2.

For the vertical polarization we obtain the characteristic NRI band of closely stacked ET hole arrays.[12] To ensure an effective negative refraction index medium along the propagation direction the holes must operate in cutoff, $f < f_{\text{cutoff}}$ or, more formally, $2a = \lambda_{\text{cutoff}} < d_y < \lambda_{\text{NRI}}$ ($a = 1.2$ mm; $f_{\text{cutoff}} = 125$ GHz for the freestanding stack and $f_{\text{cutoff}} = 80$ GHz for a stack embedded in dielectric with $\epsilon = 2.43$), and also[12] $d_z \ll \lambda_{\text{NRI}}$. Due to the quasi-self-complementariness, a single plate has an extraordinary reflection (ER) dip for the horizontal polarization.[19] Therefore, it seems reasonable that ER is the origin of the upper frequency limit of the band observed in the dispersion diagram. Ideally, ER would be located at the ET wavelength, but the dielectric loading and the multilayer stack affect differently to both polarizations, detuning the frequency of ET and ER. As shown in the diagram, we can mold the features of each polarization by changing d_x and d_y. A modification of d_y has a great impact on the location of the NRI band, whereas the positive refraction band remains unaffected. Conversely, varying d_x we adjust the PRI band without touching the NRI band. Obviously, the solution we are seeking is one in which negative and positive refraction bands overlap, like the one shown in the red curves of Fig. 2, where $d_x = 1.8$ mm and $d_y = 3.8$ mm. If we choose $d_x = 2.2$ mm (green curves) then the PRI band

moves and both curves do not intersect. Conversely, if d_y =3.3 mm, then the NRI band shifts without crossing the PRI band.

The negative and positive refraction regimes can be explained with a simplified transmission line model, as shown in a previous paper.[12] The narrow slits connecting holes barely modify the field distribution allowing ET for vertical polarization.[16] Complementarily, the narrow wires connecting patches have little effect on the ER dip.[16,19] Hence, the vertical polarization sees practically a hole array, modeled as an *L-C* tank, whereas the horizontal polarization sees a patch array, modeled as a series *L-C* circuit.[16] As a consequence of the stacking, an interplate series capacitance (electric coupling) appears in both equivalent circuits, as well as a distributed series inductance and a distributed shunt capacitance, which stem from the transmission line associated with the free space between plates. At ET, the subwavelength hole shunt inductance and the interplate series capacitance become dominant and consequently, the equivalent circuit of the stacked hole array is the dual of the conventional transmission line, i.e., a left-handed transmission line.[12] On the other hand, the series capacitance dominates in the patch array and along with the interplate series capacitance leads to a lowpass-stopband dispersion diagram.

III. EXPERIMENTAL RESULTS

The structure (see Fig. 1) was fabricated by milling the copper layer of a low-loss microwave substrate board (dielectric permittivity ε=2.43, dielectric thickness h =0.49 mm) with the following parameters: a=1.2 mm, s =0.2 mm, metal thickness t=35 μm, d_x=1.8 mm, d_y =3.8 mm, d_z=0.525 mm. An important aspect in the experiment is the fractional area occupied by the hole, which should be as large as possible to obtain a good transmission with holes still remaining in cutoff. The parameters chosen fulfil this constraint, as demonstrated in Ref. 20.

Transmission measurements were carried out using an ABmm™ quasioptical vector network analyzer in a Quasioptical Bench. The setup consists of two corrugated horn antennas (the transmitting and the receiving ones) and two pairs of elliptical mirrors. The system can be seen as a beam waveguide. The function of the primary pair of mirrors is focusing the beam so as to have an undistorted beam having its waist at the sample positioner, whereas the second set focuses the transmitted beam into the receiving antenna. The transmitter launches a vertically polarized Gaussian beam and the polarizer is rotated in its plane 45°. Hence, the *E*-field vector splits in two orthogonal components, identical in magnitude. These are detected by rotating the receiving antenna ±45°.

The experimental phase evolution is depicted in Fig. 3 for the NRI (solid lines) and PRI (dashed lines) components. Clearly, in the band between 51.5 and 58 GHz, the phase of the NRI component increases when the stack is enlarged, accounting for anomalous negative index behavior.[12] Conversely, the phase of the PRI component decreases, an evidence of positive index behavior.
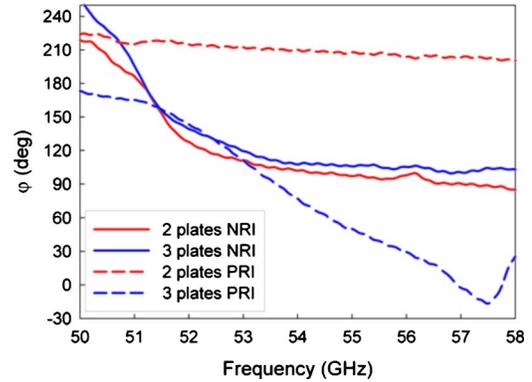

FIG. 3. (Color online) Measured phase for NRI component, two plates (solid red) and three plates (solid blue) and for the PRI component, two plates (dashed red) and three plates (dashed blue). For the NRI the phase increases between 50 and 58 GHz (anomalous behavior), whereas for the PRI the phase decreases.

The polarization selection ability is shown in Fig. 4, where, for the sake of clarity, we have depicted the ratio between the NRI and PRI components (the magnitude is in decibel scale, hence we plot the difference). For two stacked wafers [panel (a)] a LHCP is achieved at 52.1 GHz, i.e.,
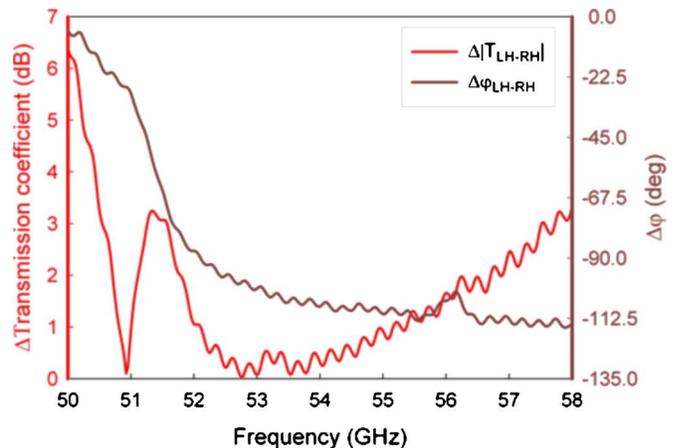
(a)
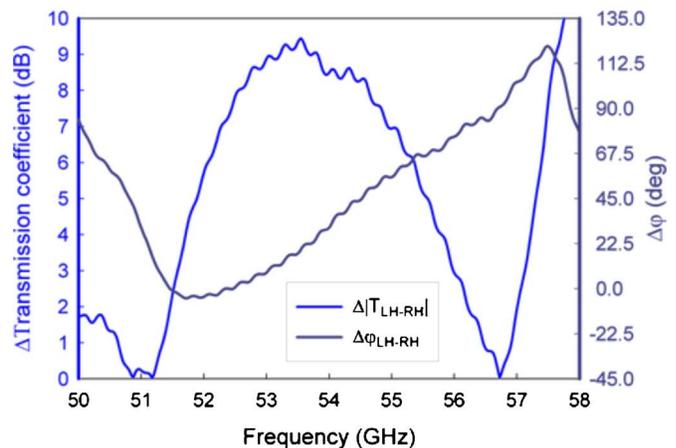
(b)

FIG. 4. (Color online) Magnitude and phase difference between the NRI and PRI transmission coefficients for (a) two stacked plates and (b) three stacked plates.

magnitude is equal and the phase difference between components is $-90°$. This frequency agrees well with the simulation results of Fig. 2, within a few percent error (inherent tolerances in the fabrication process may have caused the frequency shift). For three stacked wafers a linear polarization rotated 31° with respect to the incident polarization is obtained at the same frequency, i.e., both components are in phase.

In turn, a left-handed elliptical polarization is obtained at 50.8 GHz for two stacked wafers, whereas at this frequency the polarization becomes a right-handed elliptical polarization for three stacked wafers. Last but not least, a 45° linear polarization [in the (PRI, NRI) frame)] can be seen at 51.4 GHz for three wafers instead of the left-handed elliptical polarization that can be observed for two wafers. We have only highlighted the more obviously interesting points in the curves, but it is proven by simple inspection of the figure that many polarization states exist at other frequencies and that they also change by just increasing the number of stacked plates from 2 to 3. Needless to say, this way of proceeding can be followed until the losses become significant. Thus, if different polarization states have to be achieved, the number of stacked wafers must be increased until this constraint turns out to be remarkable.

IV. CONCLUSIONS

In conclusion, we have tailored a polarization selector involving two hot topics, namely, ET and metamaterials with negative and positive indices of refraction. We have shown that a modified hole array (or modified patch array; both points of view are equally valid) can be designed to present the required propagation characteristic, i.e., different phase constants in each polarization. From an arbitrary polarization at the input, with the only constraint of having field components along both axes that exhibit negative and positive indices of refraction, any polarization can be attained by just increasing the number of stacked plates The pioneering feature of our device is the achievement of the phase shift between components by means of a pair of orthogonal eigenwaves with negative and positive indices of refraction, respectively. Furthermore, the principles governing the proposed structure have been intuitively identified through an engineering-based lumped circuit. Experimental measurements confirm our predictions, showing polarization rotation as the structure progressively grows. The very recent proposal to introduce thin layers of liquid crystal to design near-infrared metamaterials with a reconfigurable index of refraction from negative through zero to positive values[21] opens envisaged using the concepts presented in this letter. With the given results, many applications can be envisaged, being the most obvious miniaturized polarization rotators. Also, application in LCD screens can be foreseen.

[1] S. Cornbleet, *Microwave Optics—The Optics of Microwave Antenna Design* (Academic, London, 1976).
[2] B. Z. Katsenelenbaum, *High-Frequency Electrodynamics* (Wiley-VCH, Weinheim, 2006).
[3] B. E. A. Saleh and M. C. Teich, *Fundamentals of Photonics* (Wiley, Chichester, 1991).
[4] J. A. Kong, *Electromagnetic Wave Theory* (EMW, Cambridge, MA, 2005).
[5] J. B. Pendry, Science **306**, 1353 (2004).
[6] T. W. Ebbesen, H. J. Lezec, H. F. Ghaemi, T. Thio, and P. A. Wolff, Nature (London) **391**, 667 (1998).
[7] E. Ozbay, Science **311**, 189 (2006).
[8] M. Beruete, M. Sorolla, I. Campillo, J. S. Dolado, L. Martin-Moreno, J. Bravo-Abad, and F. J. Garcia-Vidal, Opt. Lett. **29**, 2500 (2004).
[9] M. Beruete, M. Sorolla, I. Campillo, and J. S. Dolado, IEEE Microw. Wirel. Compon. Lett. **15**, 116 (2005).
[10] M. Beruete, M. Sorolla, I. Campillo, J. S. Dolado, L. Martin-Moreno, J. Bravo-Abad, and F. J. Garcia-Vidal, IEEE Trans. Antennas Propag. **53**, 1897 (2005).
[11] J. B. Pendry, L. Martin-Moreno, and F. J. Garcia-Vidal, Science **305**, 847 (2004).
[12] M. Beruete, M. Sorolla, and I. Campillo, Opt. Express **14**, 5445 (2006).
[13] M. Beruete, I. Campillo, M. Navarro-Cía, F. Falcone, and M. Sorolla, IEEE Trans. Antennas Propag. **55**, 1514 (2007).
[14] S. Zhang, W. Fan, N. C. Panoiu, K. J. Malloy, R. M. Osgood, and S. R. J. Brueck, Phys. Rev. Lett. **95**, 137404 (2005).
[15] G. Dolling, C. Enkrich, M. Wegener, C. M. Soukoulis, and S. Linden, Science **312**, 892 (2006).
[16] M. Beruete, M. Navarro-Cía, M. Sorolla, and I. Campillo, Opt. Express **15**, 8125 (2007).
[17] J. Hao, Y. Yuan, L. Ran, T. Jiang, J. A. Kong, C. T. Chan, and L. Zhou, Phys. Rev. Lett. **99**, 063908 (2007).
[18] The commercial solver CST Microwave Studio™ has been used.
[19] F. J. García de Abajo, R. Gómez-Medina, and J. J. Sáenz, Phys. Rev. E **72**, 016608 (2005).
[20] M. Beruete, M. Sorolla, M. Navarro-Cía, F. Falcone, I. Campillo, and V. Lomakin, Opt. Express **15**, 1107 (2007).
[21] D. H. Werner, D. H. Kwon, I. C. Khoo, A. V. Kildishev, and V. M. Shalaev, Opt. Express **15**, 3342 (2007).